Gynecologic Oncology 160 (2021) 450–456

Contents lists available at ScienceDirect

Gynecologic Oncology

journal homepage: www.elsevier.com/locate/ygyno

Immune cell composition in the endometrium of patients with a complete molar pregnancy: Effects on outcome

Yvonne M. Hoeijmakers [a,b,c,*], Mark A.J. Gorris [d], Fred C.G.J. Sweep [b], Johan Bulten [e], Yalck K. Eysbouts [a], Leon F.A.G. Massuger [f], Petronella B. Ottevanger [c], Jolanda I.J.M. de Vries [c,d]

[a] Department of Obstetrics and Gynecology, Radboud University Medical Center, Nijmegen, Netherlands
[b] Department of Laboratory Medicine, Radboud University Medical Center, Nijmegen, Netherlands
[c] Department of Medical Oncology, Radboud University Medical Center, Nijmegen, Netherlands
[d] Department of Tumor Immunology, Radboud Institute for Molecular Life Sciences, Radboud University Medical Center, Nijmegen, Netherlands
[e] Department of Pathology, Radboud University Medical Center, Nijmegen, Netherlands
[f] Radboud University Medical Center, Nijmegen, Netherlands

HIGHLIGHTS

- Endometrium of complete moles contains a high density of endometrium infiltrating T cells.
- NK-T cell density in endometrium of complete moles is linked to its spontaneous regression.
- The immune cell landscape in the endometrium of complete moles differs between patients with spontaneous regression and patients with progression to post-molar GTN.

ARTICLE INFO

Article history:
Received 5 September 2020
Accepted 6 November 2020
Available online 17 November 2020

Keywords:
Complete hydatidiform mole
Tumor infiltrating lymphocytes
Multiplex immunohistochemistry
Natural killer t-like cells

ABSTRACT

Objective. In 15% of patients with complete hydatidiform mole (CHM), disease progresses to post-molar gestational trophoblastic neoplasia (GTN) after curettage. Tumor infiltrating lymphocytes (TILs) are essential in overcoming disease in many tumors. Infiltrating lymphocyte composition and density may influence trophoblast regression and development of post-molar GTN. We analyzed immune cell composition and density in curettaged endometrium of patients with CHM which spontaneously regressed, and of patients with CHM which progressed to post-molar GTN.

Methods. Sixteen patients with CHM and spontaneous regression, and 16 patients with CHM which progressed to post-molar GTN were selected. Immune cell composition and density of natural killer (NK) cells, natural killer T (NKT)-like cells, Cytotoxic T cells, T-Regulatory and T-Helper cells, were determined by multiplex immunohistochemistry (mIHC).

Results. Curettaged endometrium of patients with CHM and spontaneous regression contained a slightly higher number of immune cells compared to patients with CHM which progressed to post-molar GTN. NKT-like cell density was significantly higher in patients with spontaneous regression compared to patients with CHM which progressed to post-molar GTN (483 ± 296 vs.295 ± 143 (mean $\pm$ SD), $p = 0.03$) respectively. NKT-like cell density in the spontaneous regression group was split in 'high' and 'low' (i.e. above and below the median number of NKT-like cells). In patients with high NKT-like cell density, hCG normalized earlier than in patients with low NKT-like cell density (9.5 weeks, (range 3.7–14) vs. 12.9 weeks, (range 8.6–17.9), $p = 0.05$).

Conclusion. A high number of NKT-like cells in the endometrium of CHMs may contribute to spontaneous regression of molar trophoblast cells.

1. Introduction

Gestational trophoblastic disease represents a heterogeneous group of pregnancy related disorders originating from placental tissue [1]. The most common form of gestational trophoblastic disease is the hydatidiform mole, which is subdivided in complete (CHM) and partial

* Corresponding author at: Radboud University Medical Center, Department of Obstetrics and Gynecology (internal mail 623), P.O. Box 9101, 6500HB Nijmegen, The Netherlands.
E-mail address: Y.Hoeijmakers@radboudumc.nl (Y.M. Hoeijmakers).

https://doi.org/10.1016/j.ygyno.2020.11.005

hydatidiform moles [1,2]. CHMs are diploid and androgenetic, resulting from duplication of the haploid genome of a single sperm, or dispermic fertilization of an ovum. In both cases, maternal DNA is lost, and nuclear DNA is entirely paternal [1]. In approximately 15% of all CHMs, trophoblastic activity after uterine suction curettage persists, a condition referred to as post-molar gestational trophoblastic neoplasia (GTN) [3]. Although much effort has been put into understanding the development from hydatidiform moles to GTN, the underlying mechanism is still unclear [4–6].

Immune tolerance towards the trophoblast cells still present after suction curettage could be a contributing factor to the development of post-molar GTN, since studies show that in normal pregnancies immune tolerance is essential [7–9]. In normal pregnancies, trophoblast cells expressing both maternal and paternal antigens are tolerated by the surrounding maternal immune system to sustain foetal development [7,8,10]. Trophoblast cells do not express the classical major histocompatibility (MHC) class I molecules human leukocyte antigen (HLA) -A, and —B, or MHC class II molecules, which are involved in T cell mediated recognition [9–11]. The immune checkpoint programmed death ligand 1 (PD-L1), is highly expressed on the syncitiotrophoblast and functions as an immune suppressant when bound to its receptor programmed death 1 (PD-1) [12]. In mice, a blockade or deficiency of PD-L1 resulted in decreased foetal survival rates [8]. Trophoblast cells of both hydatidiform moles and GTNs highly express PD-L1, suggesting that the PD-1/PD-L1 pathway might be involved in uncontrollable growth of these cells, leading to malignant tissue formation [13–17]. A recent study showed that anti PD-1 therapy in patients with chemo-resistant GTN was successful in three out of four treated patients [16].

In many tumor types, a high number of tumor infiltrating lymphocytes (TILs) is beneficial for clinical outcome of cancer patients. Absence or low density of TILs often results in a poor response to treatment with immune checkpoint inhibitors [16,18–21]. Trophoblast cells of CHMs display many features of malignant cells and have the potential to become malignant. Therefore, an inadequate immune response towards trophoblast cells from CHMs, may contribute to progression into post-molar GTN. Since knowledge of immune cell presence in CHMs is limited, the aim of this study was to get insight in immune cell composition and density in the curettaged endometrial tissue of patients with a CHM which spontaneously regressed after suction curettage and of patients with a CHM which progressed to post-molar GTN.

2. Methods

2.1. Patients

We selected 16 patients with complete hydatidiform moles which spontaneously regressed after suction curettage and 16 patients with complete moles which progressed to post-molar GTN. Selection was based on the availability of formalin-fixed and paraffin-embedded specimens (FFPEs) of the first curettage at the Radboud university medical center pathology archive. Sixteen samples of patients with a CHM and progression to post-molar GTN were available for further analysis. To achieve an equal amount of cases and controls, 16 samples of patients with a CHM followed by spontaneous regression were included. Follow-up data was retrieved from the Dutch Central Registry for Hydatidiform Moles (DCRHM). Patient data are collected in this voluntary registry since 1977. For patients with spontaneous regression, the minimum follow-up period after normalization was six months. For patients diagnosed with post-molar GTN, follow-up was one year after normalization of hCG levels. No patients of the spontaneous regression or post-molar GTN group showed signs of intra-uterine retention of trophoblast tissue. Patients with a history of auto-immune diseases, recurrent hydatidiform moles or with no treatment data available were excluded. Post-molar GTN was defined according to the FIGO 2000 guideline (i.e., mola hydatidosa with serum hCG plateauing for three consecutive weeks or rising over a period of two consecutive weeks) [22]. In line with the Dutch guidelines, the following criterion was added to this definition: at least one of the values should exceed the 95th percentile of an hCG normogram of uneventful hCG as constructed by Yedema et al. [23]. The local ethical committee of the Radboud University Medical Center approved this study (reference number **2018–4132**).

2.2. Multiplex immunohistochemistry

Of each selected patient, hematoxylin-eosin (HE) slides of all available FFPE specimens, varying from 2 to 8 tissue blocks, were assessed for the presence of both endometrial and implantation trophoblast tissue by an experienced gyneco-pathologist. The selected FFPE specimens of the 32 selected patients were cut in sequential sections of 4-μm thickness and mounted on glass slides. Control slides included tonsil, colon, liver and pancreatic tissue [24]. One slide was subjected to hematoxylin-eosin (HE) staining, and specific endometrial and trophoblast regions were indicated by an experienced gyneco-pathologist. Another slide was subjected to seven-color multiplex immunohistochemistry (mIHC) in sequential staining cycles using Opal 7-color Automation IHC Kit (NEL801001KT; PerkinElmer) on the BOND RX IHC & ISH Research Platform (Leica Biosystems). A multiplex panel for the detection of different lymphocyte populations was optimized as described before [25] and applied on tissue sections, consisting of anti-CD45RO 1:1000 (MS-112, clone UCHL-1; Thermo Scientific) with Opal 620, anti-CD8 1:200 (M7103, clone C8/144B; Dako) with Opal 690, anti-CD3 1:200 (RM-9107, clone Sp7; Thermo Fisher) with Opal 520, anti-Foxp3 1:100 (14–4777, clone 236A/E7; eBioscience Affymetrix) with Opal 540 anti-CD56 1:500 (156R-94, clone MRQ-42; Cell Marque) with Opal 570, and anti-pan Cytokeratin 1:1500 (ab86734, clone AE1/AE3 + 5D3; Abcam) with Opal 650. Primary antibody incubations were performed for 1 h, secondary antibody Opal Polymer HRP Ms. + Rb incubations for 30 min, and Opal reagent incubations for 10 min, all at room temperature. All epitope retrievals and antibody-TSA complex removals were performed using Bond Epitope Retrieval 2 (AR9640, Leica Biosystems). Tissue sections were counterstained with DAPI and mounted in Fluoromount-G (0100–01, SouthernBiotech, Birmingham, AL, USA).

The slides were scanned using the Vectra Automated Quantitative Pathology Imaging System (Version 3.0.4, PerkinElmer). In each sample, the endometrial tissue was selected using Phenochart (Version 1.0.9, PerkinElmer Inc.), for multispectral imaging at 20× magnification, based on HE slides annotated by the gyneco-pathologist. Only endometrial regions were analyzed, since no immune cell infiltration was detected in trophoblast. Spectral unmixing of Opal fluorophores, DAPI, autofluorescence, and downstream image analysis was performed with inForm software (Version 2.2.1, PerkinElmer). The pathologist and researchers were blinded to patient follow-up details during the staining, scanning and analysis period.

A selection of 30–35 representative original multispectral images were used to train the inForm software to distinguish hemorrhagic endometrial tissue from non-hemorrhagic endometrial tissue, trophoblast tissue, and background, based on DAPI and autofluorescence. Settings for adaptive cell segmentation were based on DAPI and membrane signals. All the settings applied to the training images were saved in an algorithm to allow batch analysis of multiple original multispectral images of the same CHM slides.

2.3. Image cytometry

Segmented cell data was converted into Flow Cytometry Standard (FCS) files, and analyzed using FlowJo software (v10; Tree Star). Phenotype of the immune cells in non-hemorrhagic endometrial tissue regions were determined by gating cells and divided by surface area of the tissue region (mm^2).

2.4. Statistical analysis

As data were not normally distributed, we used the Mann-Whitney *U* test to compare baseline characteristics between the spontaneous regression and post-molar GTN group. Immune cell density of the immune phenotypes was calculated per mm^2 non-hemorrhagic endometrial tissue, and means were compared with the two-sided Students *t*-test when data was normally distributed after log-transformation. When after log-transformation data was skewed we used the Mann-Whitney *U* test. A *p*-value of ≤0.05 was considered significant. In this hypothesis-generating study, we did not correct for multiple testing.

3. Results

Baseline characteristics of the included patients are displayed in Table 1. There was no difference between both groups in terms of patients' age, and gestational age at diagnosis. Pre-evacuation serum hCG levels tended to be higher in the post-molar GTN group, although not significant ($p = 0.06$). Samples of the post-molar GTN group contained more hemorrhagic tissue within the imaged tissue areas compared to samples of the spontaneous regression group (Table 1). We selected endometrial tissue regions for multispectral imaging at a 20× magnification (Fig. 1A and —B). Different immune cell populations were detected within samples (Fig. 1C). Non-hemorrhagic tissue could adequately be separated from hemorrhagic tissue and background by tissue segmentation with inForm (Fig. 1D). Only non-hemorrhagic endometrial tissue was included in the analysis. Single cell information was transformed into FCS files and further analyzed using image cytometry (Fig. 2). We calculated immune cell density per mm^2 non-hemorrhagic endometrial tissue in both groups for natural killer (NK) cells ($CD56^+$), natural killer T (NKT)-like cells ($CD56^+$, $CD3^+$), total T cells (Cytotoxic T cells + T regs + NKT-like cells + T helper cells), cytotoxic T cells ($CD8^+$), T-helper cells ($CD8^-$, $FOXP3^-$, $CD3^+$), and T-regulatory cells ($FOXP3^+$), (Fig. 3). T cell populations were not further divided into CD45RO positive and negative, since no reliably discrimination between these populations was possible. Therefore, the CD45RO marker was excluded from the analysis.

In general, the curettaged non-hemorrhagic endometrial tissue of patients with a CHM and spontaneous regression contained a slightly higher number of total $CD3^+$ immune cells compared to the curettaged non-hemorrhagic endometrial tissue of patients with CHM which progressed to post-molar GTN (Fig. 3). Median density of cytotoxic T cells, T helper cells, and T regulatory cells were similar in both groups (Fig. 3). Although not significant, the number of NK cells observed in the spontaneous regression group, tended to be higher than the number of NK cells in the post-molar GTN group. Non-hemorrhagic curettaged endometrial tissue of patients with CHM and spontaneous regression after curettage had a significantly higher number of NKT-like cells per mm^2 compared to endometrial tissue of patients which progressed to post-molar GTN (483 ± 296 versus 295 ± 143 (mean ± SD) NKT-like cells per mm^2, respectively, $p = 0.03$), (Fig. 3).

To investigate the relevance of a higher number of NKT-like cells in the curettaged endometrial tissue of CHM patients for clinical outcome, each of the two patient populations (i.e. patients with a CHM which spontaneously regressed after suction curettage, and patients with a CHM which progressed to post-molar GTN), were divided in NKT-like cell density above and below the median density. There was no correlation between pre-evacuation hCG level and NKT-like counts. (Pearson correlation −0.57, $p = 0.11$). In patients with CHM and spontaneous regression after curettage, who had an NKT-like cell infiltrate in the endometrial tissue above the median, mean time until hCG normalization took 9.5 weeks (±3.0) compared to 12.9 weeks (±3.3) in patients with an NKT-like cell density below the median ($p = 0.05$), (Fig. 4). In patients with a CHM which progressed to post-molar GTN, and therefore treated with methotrexate (MTX) chemotherapy, mean number of MTX courses needed until hCG normalization was 6.3 (±3.9) in patients with an NKT-like cell density above the median, and 7.4 (±4.6) in patients with an NKT-like cell density below the median, ($p = 0.77$).

4. Discussion

4.1. Main findings

Significantly more $CD3^+CD56^+$ NKT-like cells were present in the endometrium of patients with a CHM and spontaneous regression, compared to patients with a CHM which progressed to post-molar GTN (Mean ± SD 483 ± 296 versus 295 ± 143 cells per mm^2, respectively, $p = 0.03$). Also, patients in the spontaneous regression group tended to normalize earlier when NKT-like cell infiltrate in the endometrium was above the group median (mean 9.5 weeks, ±3.0) compared to patients with a NKT-like cell infiltrate below the group median (mean 12.9 weeks, ±3.3), $p = 0.05$. These observations may indicate that NKT-like cells influence spontaneous regression of CHMs after curettage.

4.2. Strengths and limitations

This study is the first to use seven-color mICH to simultaneously quantify different immune cells within the curettaged endometrial tissue of patients with a CHM. With this technique, we were able to analyze presence and density of five immune cell phenotypes within one sample, and link trophoblast regression to density of NKT-like cells. Another advantage of this technique is that it offers detailed information regarding distribution of immune cell phenotypes, while maintaining the morphological context of the tissue. Although selection of the analyzed samples was based on presence of endometrial and implantation trophoblastic tissue, retrieval of these samples was through uterine curettage. Therefore, we were unable to apprehend the exact approximity of the endometrial tissue to the trophoblast cells. Although a large part of the analyzed endometrial tissue will be representative of the decidua basalis and capsularis located at the implantation site, a part of the measured immune cell populations might be representative of the decidua parietalis. This however is true for all samples used in this study and may have had an equal influence on both the spontaneous regression, and the post-molar GTN group. Additionally, uterine suction curettage

Table 1
Baseline characteristics of patients with CHM and a spontaneous regression after curettage and patients with post-molar GTN[a].

	Spontaneous regression	Post-molar GTN	*p*-value
	N Median (min – max)	N Median (min – max)	
Age at time diagnosis (years)	16 31 (20–54)	16 31 (20–52)	0.86[b]
Gestational age (weeks)	10 11 (7–18)	13 11 (9–24)	0.79[b]
Pre-evacuation hCG level (ng/mL)	6 2,700 (610–5300)	8 5,649 (2550–16,000)	0.06[b]
Analyzed non-hemorrhagic tissue (mm^2)	16 26 (2–138)	16 19 (1–37)	0.31[b]
Hemorrhagic tissue (mm^2)	16 2 (0–4)	16 3 (0–7)	0.01[b,c]

[a] Data shown for all patients with baseline features available.
[b] Mann-Whitney *U* test.
[c] Significant at $p < 0.05$ level.

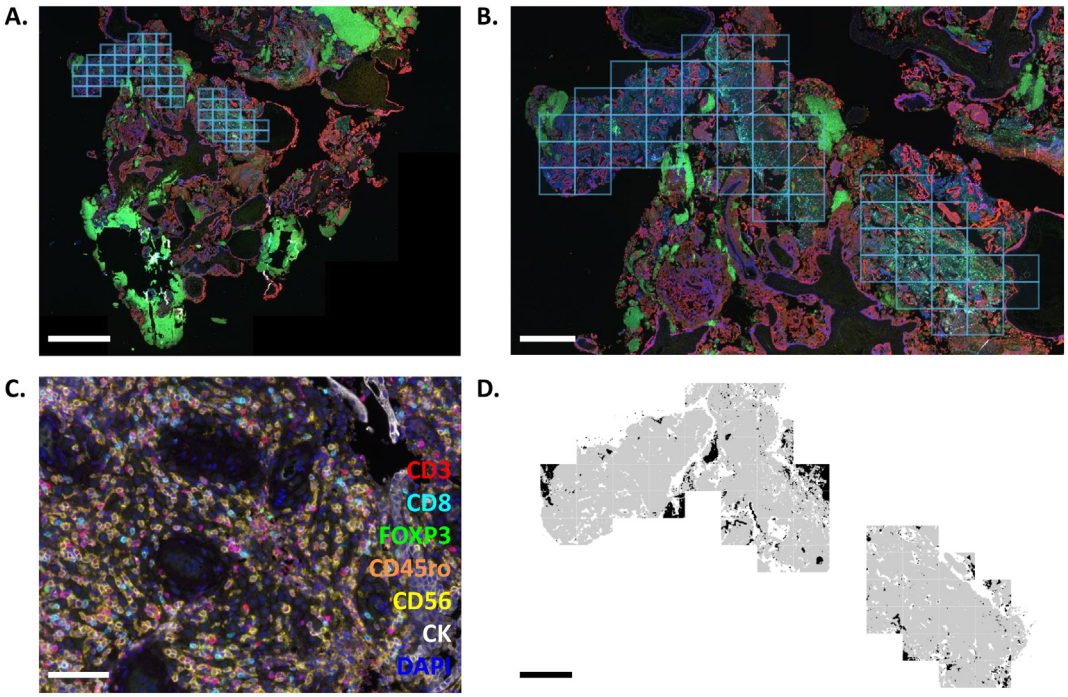

Fig. 1. Multiplex immunohistochemistry of curettaged endometrial tissue of a patient with a CHM. Slides were stained with a lymphocyte panel containing CD3, FOXP3, CD8, CD56, CD45ro, pan-cytokeratin (CK) and DAPI, and scanned with the Vectra 3. A and B) Regions of endometrial tissue were selected for multispectral images (MSIs) at 20× magnification (light-blue rectangles) from the prescans (using DAPI, FITC and Cy5 filters) within Phenochart. From these overviews DAPI (blue), CD3 (green), CK (red) and autofluorescence coming from hemorrhagic tissue areas (green) are mainly visible. Scale bars are 3 and 1 mm, respectively. C) Composite image from unmixed MSIs using inForm Cell Analysis software, visualizing CD3 (red), CD8 (cyan), FOXP3 (green), CD45ro (orange), CD56 (yellow), pan-CK (white) and DAPI (blue) at 20× magnification. Scale bar is 0.1 mm. D) Overview of batch-analyzed tissue segmentation dividing the tissue into "non-hemorrhagic endometrial tissue" (grey) and "hemorrhagic endometrial tissue" (black) regions. Only the areas of non-hemorrhagic endometrial tissue were analyzed. Scale bar is 1 mm.

is the least invasive manner to remove a molar pregnancy, and all retrospective and future samples most probably will be collected in this manner.

Because post-molar GTN is rare, we were limited by a retrospective design and a relatively small sample size. Differences in absolute NK cell numbers may exist between the spontaneous regression and post-molar GTN group, but our study may have been underpowered to detect this difference. This also may apply for the role of NKT-like cells in the clearance of CHMs in combination with chemotherapy. Unlike most malignant diseases, diagnosis of post-molar GTN is currently based on clinical parameters, i.e. level and course of serum hCG, instead of confirmation by histology [1,22]. To ensure diagnosis of post-molar GTN is not erroneously based on a missed uterine retention, macroscopic complete removal of the molar pregnancy was confirmed during or after the initial uterine curettage.

4.3. Interpretation

The most prevalent cell type within the endometrial tissue of CHM patients were the $CD56^{+}$ NK cells. This cell type is also the most abundant in the decidua of normal pregnancies, representing 70% of the leukocytes present *in utero*[26]. Of the two subpopulations of NK cells present in normal pregnancies: $CD56^{dim}$ $CD16^{+}$, and $CD56^{bright}$ $CD16^{-}$, the majority of decidual NK cells (dNK cells) consists of the less cytotoxic $CD56^{brigh}$t

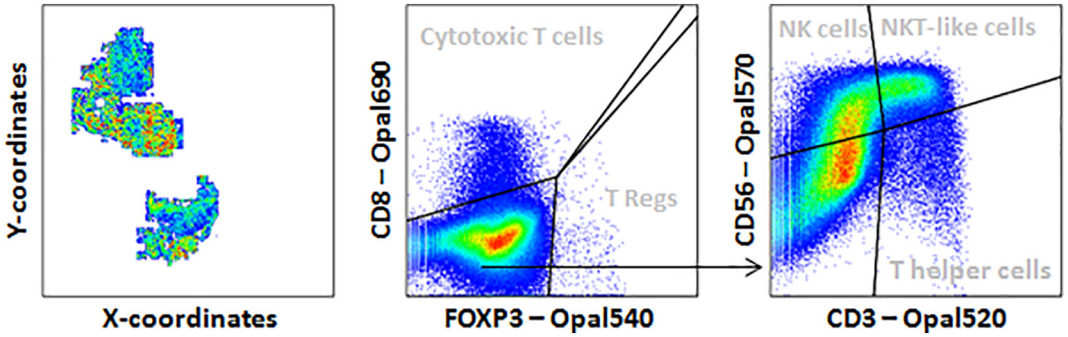

Fig. 2. Image cytometry gating strategy. Cells were segmented using in Form Cell Analysis software based on DAPI and FOXP3 as nuclear signals, and splitted using membrane signals. Single cell information was transformed into an.fcs file and further analyzed using image cytometry within Flow Jo. In the left panel, single cell events within the intact tissue are visualized in its spatial context. In the middle panel, CD8 positive and FOXP3 positive cells are gated out from the sample. In the right panel, cells negative for CD8 and FOXP3 are further gated for CD56 positivity and/or CD3 positivity. From here different phenotypes were extracted: NK cells ($CD56^{+}$), NKT-like cells ($CD56^{+}$,$CD3^{+}$), Cytotoxic T cells ($CD8^{+}$), T-regulatory cells ($FOXP3^{+}$), T-helper cells ($CD56^{-}$, $CD8^{-}$, $FOXP3^{-}$, $CD3^{+}$), and total T cells (Cytotoxic T cells + T regs + NKT-like cells + T helper cells). This figure represents the gating of one of the samples used in this study.

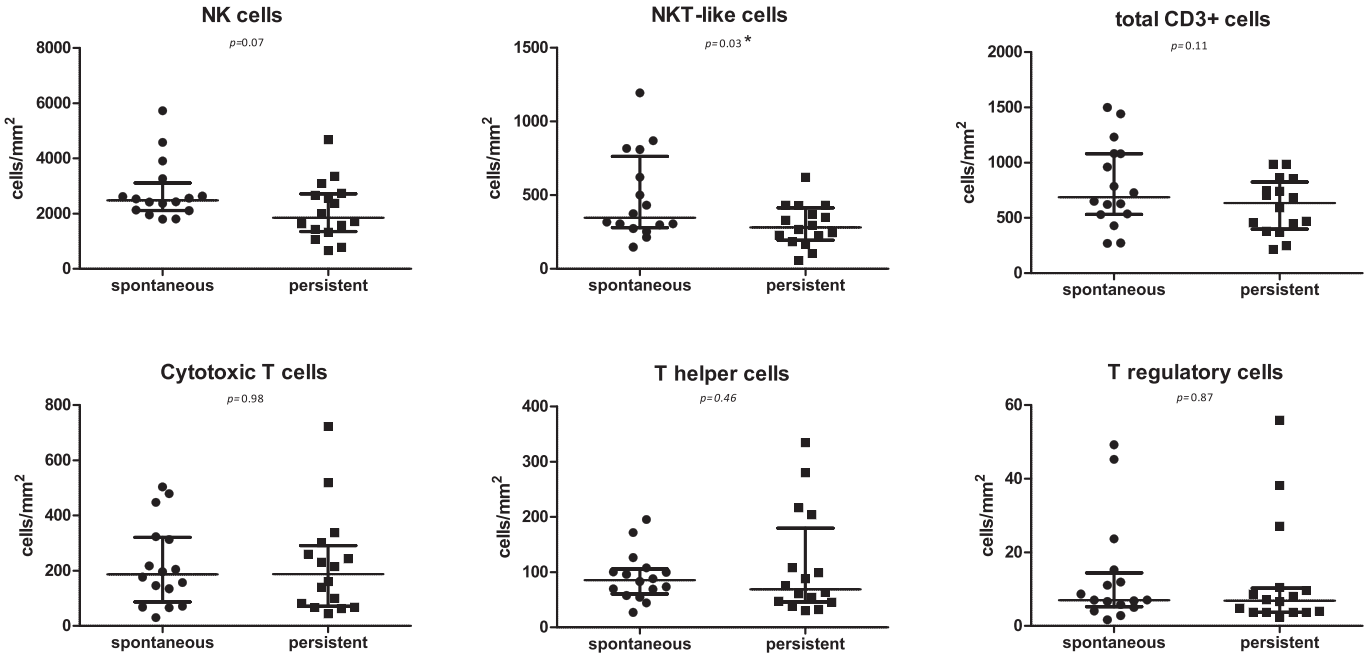

Fig. 3. Number of immune cells present per mm^2 in endometrial tissue of patients with CHM and a spontaneous regression after curettage (spontaneous) and patients with post-molar GTN (persistent). Lines display median with IQ-range. *Significant at the $p \leq 0.05$ level.

CD16$^-$ phenotype [10]. The origin of these dNK cells is still unclear. Possibly, NK cells are recruited from other organs or from peripheral blood to the decidua, where they undergo tissue-specific differentiation. Another theory is that dNK cells originate from hematopoietic progenitor cells or endometrial NK cells residing in the endometrium, which proliferate and differentiate into dNK cells during early pregnancy [27]. Regardless, dNK cells are thought to play an important role in pregnancies, promoting uterine vascular change, necessary for maternal blood flow through the placenta [26]. In the pre-malignant CHM, the role of dNK cells might be different. Biologically, NK cells respond to tumor

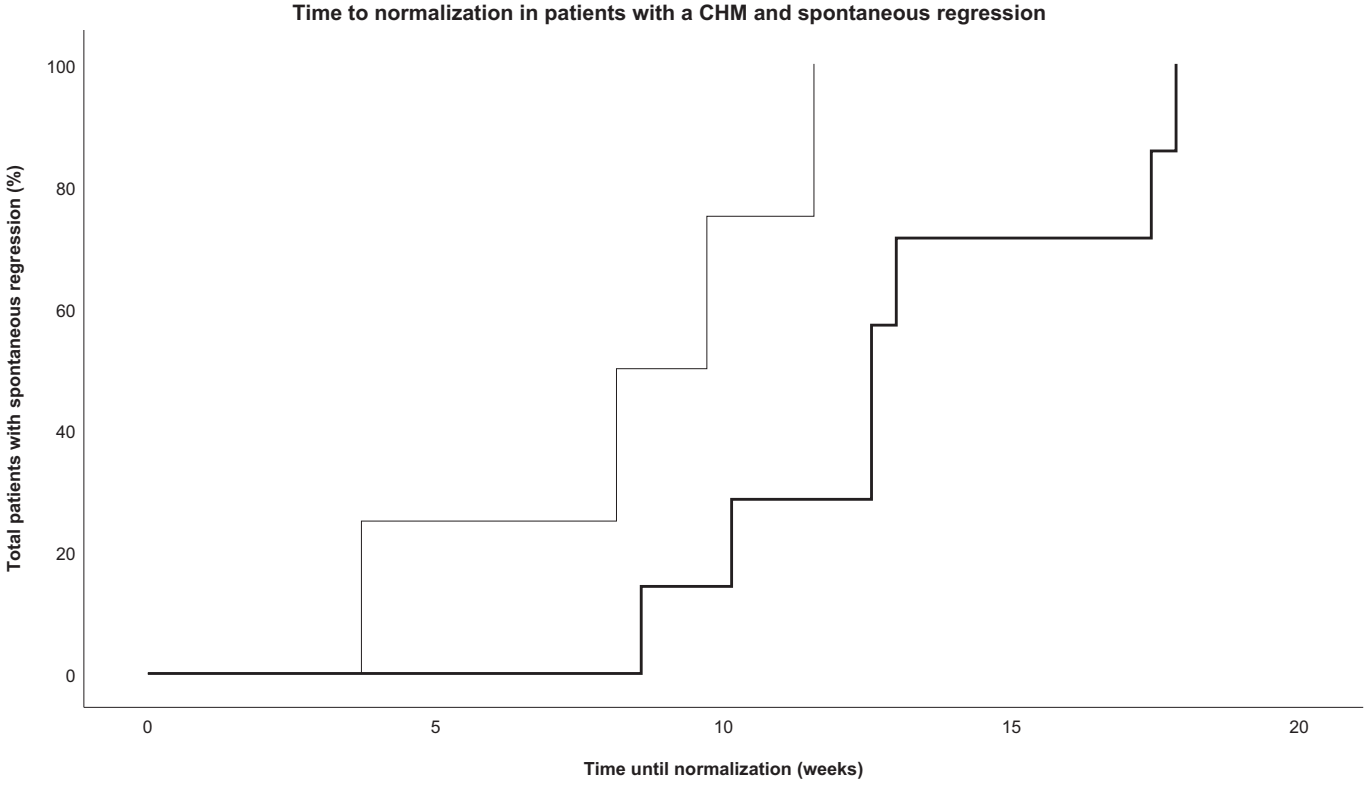

Fig. 4. Time until normalization in patients with a CHM and spontaneous regression after suction curettage. Thin line represents patients with number of NKT cells above the median, thick line represents patients with number of NKT cells below the median.

formation by killing MHC class I negative cells. Indeed, trophoblast cells lack the classical MHC class I molecules HLA-A and —B, they however do express HLA—C, HLA-E and HLA-G. HLA-C is the most dominant ligand for killer-cell immunoglobulin-like receptors (KIR), expressed by NK cells. Interaction between these receptors and ligands results in inhibition of cytotoxic functions of NK cells [9,11,28]. NK cell function is furthermore inhibited following interactions with HLA-E and HLA-G [26,29]. Although these interactions might result in NK cell tolerance towards proliferating trophoblast cells, conversely, reduced HLA-G expression was recently linked to monochemotherapy resistance of gestational choriocarcinomas [30]. Therefore, the exact role of NK cells in endometrial tissue of CHM patients remains to be elucidated.

$CD3^+CD56^+$ NKT-like cells were the second most prevalent cell type within the endometrial tissue of CHM patients. They represent a heterogeneous group of T cells, consisting of a number of diverse T cell subsets, including classical NKT cells [31–33]. In normal pregnancies, ~0.5% of the decidual $CD3^+$ T cell population are classical NKT, a frequency 10 times higher than observed in peripheral blood [31]. Classical NKT cells are characterized by the expression of both T and NK cell markers. They differ from conventional T cells in the recognition of antigens [34]. Antigen recognition in NKT cells occurs via lipids presented by CD1d, a non-classical MHC class-I-like molecule, whereas T cells detect antigens presented by conventional MHC molecules [35]. As CD1d is expressed by villous and extravillous trophoblast cells, NKT cells might play a role in trophoblast regression [31,36]. In mice, activated NKT cells have a dramatic impact on pregnancy, resulting in early or mid-gestation pregnancy loss and pre-term birth [37]. Additionally, NKT cells may be able to modulate uterine NK cell function through transactivation [34]. A study in pregnant mice showed, when NKT cells were activated through administration of αGalCer, that dNK cells became activated and produced IFN-gamma within hours of NKT cell activation. Whether this mechanism is crucial in mediating NKT-cell induced pregnancy loss is unknown. However, it demonstrates that NKT-cell function is capable of modulating dNK cell function, and that NKT cells are important in coordinating functional interactions among decidual leukocytes at the maternal-fetal interface [33,34]. Although due to the design of this study we mainly identified NKT-like cells, from which only a fraction are classical CD1d restricted NKT cells, theoretically, a higher number of NKT-like cells means a higher number of classical NKT cells. However, there are two types of NKT cells which have distinct and opposing roles. Type I NKT cells mainly promote immune reactions against tumor cells and produce cytokines to activate NK and cytotoxic T cells, whereas type II NKT cells are known to inhibit tumor directed immune reactions [33,34]. The immune function of NKT cells, either pro-inflammatory or tolerogenic, depends on tissue type and presence of many other immune cells [33,35,38,39]. Thus, NKT cells present in endometrium of CHMs might be activated or suppressed due to factors derived from trophoblastic cells and surrounding endometrium. Nevertheless, in our study, increased density of NKT-like cells was associated with a greater occurrence of spontaneous regression. We might therefore suggest that a predominant fraction of the NKT-like cells excerted the classical immune stimulating NKT cell function. To further elucidate the underlying biology of NKT cells present in the decidua of patients with trophoblastic disease, future studies should focus on the identification of classical and non-classical NKT cells through the use of αGalcer loaded CD1d multimers. Density of the present classical and non-classical NKT cells may be compared between different types of trophoblastic disease and their relation to pre-evacuation hCG levels, time to normalization, and courses of chemotherapy needed.

Similar to the cellular composition of the decidua during normal pregnancies, approximately 20% of leukocytes present in the curettaged endometrium in this study are $CD3^+$ T cells, and of these $CD3^+$ cells, ~70% are $CD8^+$ cytotoxic T cells, and ~30% are $CD4^+$ T helper cells [26]. We observed no significant differences in density of these immune cells between the CHM groups. In normal pregnancies, about 5% of the $CD4^+$ are $FOXP3^+$ regulatory T cells [26]. We observed very low numbers of $FOXP3^+$ T regulatory cells within the endometrial tissue of patients in both CHM groups. As chromosomes of CHMs are entirely of paternal origin, a strong maternal immune response against these trophoblast cells would be expected [1]. Nevertheless, trophoblast cells of CHMs are able to proliferate and invade maternal tissue, suggesting a strong local immune tolerance towards these cells. Immune tolerance induced by $FOXP3^+$ T regulatory cells could be a mechanism. However, in line with our results, other studies showed low numbers of $FOXP3^+$ T regulatory cells in the endometrium of CHMs, or observed $FOXP3^+$ T regulatory cells only in association with extremely high numbers of T effector cells [20,40]. Additionally, at the implantation site of normal pregnancies, $FOXP3^+$ T regulatory cells are nearly absent [40]. Therefore, $FOXP3^+$ T regulatory cells may have no primary role in local protection of trophoblast cells in normal- and molar pregnancies.

5. Conclusion

The expression of immune checkpoint molecules, lack of classical MHC class I and MHC class II complexes, and low density of immune stimulating tumor infiltrating lymphocytes may all contribute to a tolerogenic environment within molar pregnancies and GTN. Conversely, presence of a high number of NKT-like cells may prevent malignant cell formation and contribute to tumor regression. This hypothesis should be tested in additional research with the ultimate aim to identify patients at risk of progression to post-molar GTN at an early stage. The immune microenvironment is an extensive web where the balance between immune stimulating and suppressive factors will probably decide whether a CHM wil regress or progress to post-molar GTN. Although we observed differences in immune cell composition and density between the spontaneous regression and post-molar GTN groups, prediction of persistance based on the number of the analyzed immune cells present solely, is currently not possible.

Contribution to authorship

All authors have been involved in the study design, including the conceptualization and methodology of this study. YMH, MG, and JB collected the data, YMH, MG, and JB, anlyzed and investigated/interpreted the data. FCGJS, PBO, LFAGM and IJMV supervised this process and took care of the funding acquisition. YMH wrote the original draft of the manuscriptorig orand all authors were equally involved in reviewing and editing the manuscript.

Details of ethical approval

This study was approved by the local ethical committee of the Radboud University Medical Center (reference number **2018–4132**).

Funding

This study did not receive any specific grant from funding agencies in the public, commercial, or non-for-profit sectors. MG was supported by NWO-Vici 916.14.655 awarded to IJMV.

Declaration of Competing Interest

The authors have nothing to disclose.

Acknowledgements

Authors report no acknowledgements.

References

[1] J.R. Lurain, Gestational trophoblastic disease I: epidemiology, pathology, clinical presentation and diagnosis of gestational trophoblastic disease, and management of hydatidiform mole, Am. J. Obstet. Gynecol. 203 (6) (2010) 531–539.

[2] M.J. Seckl, N.J. Sebire, R.S. Berkowitz, Gestational trophoblastic disease, Lancet (London, England) 376 (9742) (2010) 717–729.
[3] R.S. Berkowitz, D.P. Goldstein, Clinical practice. Molar pregnancy, N. Engl. J. Med. 360 (16) (2009) 1639–1645.
[4] F.T.C. Asmar, A.R. Braga-Neto, J. de Rezende-Filho, J.M.S. Villas-Boas, R.C. Charry, I. Maesta, Uterine artery doppler flow velocimetry parameters for predicting gestational trophoblastic neoplasia after complete hydatidiform mole, a prospective cohort study, Clinics (Sao Paulo, Brazil) 72 (5) (2017) 284–288.
[5] P. Zhao, S. Wang, X. Zhang, W. Lu, A novel prediction model for postmolar gestational trophoblastic neoplasia and comparison with existing models, Intern. J. Gynecol.Ccancer: Off. J. Intern. Gynecol. Cancer Soc. 27 (5) (2017) 1028–1034.
[6] M. Alazzam, T. Young, R. Coleman, B. Hancock, D. Drew, P. Wilson, et al., Predicting gestational trophoblastic neoplasia (GTN): is urine hCG the answer? Gynecol. Oncol. 122 (3) (2011) 595–599.
[7] E.S. Taglauer, A.S. Trikhacheva, J.G. Slusser, M.G. Petroff, Expression and function of PDCD1 at the human maternal-fetal interface, Biol. Reprod. 79 (3) (2008) 562–569.
[8] I. Guleria, A. Khosroshahi, M.J. Ansari, A. Habicht, M. Azuma, H. Yagita, et al., A critical role for the programmed death ligand 1 in fetomaternal tolerance, J. Exp. Med. 202 (2) (2005) 231–237.
[9] R. Hackmon, L. Pinnaduwage, J. Zhang, S.J. Lye, D.E. Geraghty, C.E. Dunk, Definitive class I human leukocyte antigen expression in gestational placentation: HLA-F, HLA-E, HLA-C, and HLA-G in extravillous trophoblast invasion on placentation, pregnancy, and parturition, Am. J. Reprod. Immunol. (New York, NY: 1989) 77 (6) (2017).
[10] A. Trundley, A. Moffett, Human uterine leukocytes and pregnancy, Tissue Antigens 63 (1) (2004) 1–12.
[11] A. Blaschitz, H. Hutter, G. Dohr, HLA class I protein expression in the human placenta, Early Pregnancy 5 (1) (2001) 67–69.
[12] S.L. Topalian, C.G. Drake, D.M. Pardoll, Immune checkpoint blockade: a common denominator approach to cancer therapy, Cancer Cell 27 (4) (2015) 450–461.
[13] P.A. Bolze, S. Patrier, J. Massardier, T. Hajri, F. Abbas, A.M. Schott, et al., PD-L1 expression in premalignant and malignant Trophoblasts from gestational trophoblastic diseases is ubiquitous and independent of clinical outcomes, Intern. J. Gynecol. Cancer: Off. J. Intern. Gynecol Cancer Soc. 27 (3) (2017) 554–561.
[14] E. Veras, R.J. Kurman, T.L. Wang, I.M. Shih, PD-L1 expression in human placentas and gestational trophoblastic diseases, Intern. J. Gynecol. Pathol.: Off. J. Intern. Soc. Gynecol. Pathol. 36 (2) (2017) 146–153.
[15] S. Inaguma, Z. Wang, J. Lasota, M. Sarlomo-Rikala, P.A. McCue, H. Ikeda, et al., Comprehensive Immunohistochemical study of programmed cell death ligand 1 (PD-L1): analysis in 5536 cases revealed consistent expression in trophoblastic tumors, Am. J. Surg. Pathol. 40 (8) (2016) 1133–1142.
[16] E. Ghorani, B. Kaur, R.A. Fisher, D. Short, U. Joneborg, J.W. Carlson, et al., Pembrolizumab is effective for drug-resistant gestational trophoblastic neoplasia, Lancet (Lond., Engl.) 390 (10110) (2017) 2343–2345.
[17] Benoit You, Pierre-Adrien Bolze, et al., Avelumab in patients with gestational trophoblastic tumors resistant to monochemotherapy: Final outcomes of TROPHIMMUN phase II trial, cohort A, J. Clin. Oncol. 38 (18_suppl) (2020) LBA6008-LBA6008.
[18] A.I. Daud, K. Loo, M.L. Pauli, R. Sanchez-Rodriguez, P.M. Sandoval, K. Taravati, et al., Tumor immune profiling predicts response to anti-PD-1 therapy in human melanoma, J. Clin. Invest. 126 (9) (2016) 3447–3452.
[19] P.C. Tumeh, C.L. Harview, J.H. Yearley, I.P. Shintaku, E.J. Taylor, L. Robert, et al., PD-1 blockade induces responses by inhibiting adaptive immune resistance, Nature 515 (7528) (2014) 568–571.
[20] Z. Nagymanyoki, M.J. Callahan, M.M. Parast, V. Fulop, S.C. Mok, R.S. Berkowitz, Immune cell profiling in normal pregnancy, partial and complete molar pregnancy, Gynecol. Oncol. 107 (2) (2007) 292–297.
[21] Z. Nagymanyoki, D. Kindelberger, R. Clark, N. Rodriguez, V. Fulop, R.S. Berkowitz, Age related cellular immune response against complete molar pregnancy, J. Reprod. Med. 55 (5–6) (2010) 261–266.
[22] FIGO staging for gestational trophoblastic neoplasia, FIGO oncology committee, Intern. J. Gynaecol. Obstetrics: Off. Organ Intern. Feder. Gynaecol. Obstetrics 77 (3) (2000) 285–287.
[23] K.A. Yedema, R.H. Verheijen, P. Kenemans, C.P. Schijf, G.F. Borm, M.F. Segers, et al., Identification of patients with persistent trophoblastic disease by means of a normal human chorionic gonadotropin regression curve, Am. J. Obstet. Gynecol. 168 (3 Pt 1) (1993) 787–792.
[24] E.C. Stack, P.G. Foukas, P.P. Lee, Multiplexed tissue biomarker imaging, J. Immunother. Cancer 4 (2016) 9.
[25] M.A.J. Gorris, A. Halilovic, K. Rabold, A. van Duffelen, I.N. Wickramasinghe, D. Verweij, et al., Eight-color multiplex immunohistochemistry for simultaneous detection of multiple immune checkpoint molecules within the tumor microenvironment, J. Immunol. 200 (1) (2018) 347–354 (Baltimore, Md: 1950).
[26] A. Erlebacher, Immunology of the maternal-fetal interface, Annu. Rev. Immunol. 31 (2013) 387–411.
[27] I. Manaster, O. Mandelboim, The unique properties of uterine NK cells, Am. J. Reprod. Immunol. 63 (6) (2010) 434–444 (New York, NY: 1989).
[28] O. Chazara, S. Xiong, A. Moffett, Maternal KIR and fetal HLA-C: a fine balance, J. Leukoc. Biol. 90 (4) (2011) 703–716.
[29] R. Apps, L. Gardner, A. Moffett, A critical look at HLA-G, Trends Immunol. 29 (7) (2008) 313–321.
[30] P.A. Bolze, J. Lopez, F. Allias, T. Hajri, S. Patrier, M. Devouassoux-Shisheboran, et al., Transcriptomic and immunohistochemical approaches identify HLA-G as a predictive biomarker of gestational choriocarcinoma resistance to monochemotherapy, Gynecol. Oncol. 158 (3) (2020 Sep) 785–793, https://doi.org/10.1016/j.ygyno.2020.05.042 Epub 2020 Jun 5. PMID: 32513563.
[31] J.E. Boyson, B. Rybalov, L.A. Koopman, M. Exley, S.P. Balk, F.K. Racke, et al., CD1d and invariant NKT cells at the human maternal-fetal interface, Proc. Natl. Acad. Sci. U. S. A. 99 (21) (2002) 13741–13746.
[32] C.H. Kim, B. Johnston, E.C. Butcher, Trafficking machinery of NKT cells: shared and differential chemokine receptor expression among V alpha 24(+)V beta 11(+) NKT cell subsets with distinct cytokine-producing capacity, Blood 100 (1) (2002) 11–16.
[33] J.E. Boyson, I. Aktan, D.A. Barkhuff, A. Chant, NKT cells at the maternal-fetal interface, Immunol. Investig. 37 (5) (2008) 565–582.
[34] M. Terabe, J.A. Berzofsky, The role of NKT cells in tumor immunity, Adv. Cancer Res. 101 (2008) 277–348.
[35] M. Terabe, J.A. Berzofsky, Tissue-specific roles of NKT cells in tumor immunity, Front. Immunol. 9 (2018) 1838.
[36] H.J. Jenkinson, S.D. Wainwright, K.L. Simpson, A.C. Perry, P. Fotiadou, C.H. Holmes, Expression of CD1D mRNA transcripts in human choriocarcinoma cell lines and placentally derived trophoblast cells, Immunology 96 (4) (1999) 649–655.
[37] J.E. Boyson, N. Nagarkatti, L. Nizam, M.A. Exley, J.L. Strominger, Gestation stage-dependent mechanisms of invariant natural killer T cell-mediated pregnancy loss, Proc. Natl. Acad. Sci. U. S. A. 103 (12) (2006) 4580–4585.
[38] N.Y. Crowe, J.M. Coquet, S.P. Berzins, K. Kyparissoudis, R. Keating, D.G. Pellicci, et al., Differential antitumor immunity mediated by NKT cell subsets in vivo, J. Exp. Med. 202 (9) (2005) 1279–1288.
[39] T. Tachibana, H. Onodera, T. Tsuruyama, A. Mori, S. Nagayama, H. Hiai, et al., Increased intratumor Valpha24-positive natural killer T cells: a prognostic factor for primary colorectal carcinomas, Clin. Cancer Res.: Off. J. Am. Assoc. Cancer Res. 11 (20) (2005) 7322–7327.
[40] Y.T. Sundara, E.S. Jordanova, B.S. Hernowo, S. Gandamihardja, G.J. Fleuren, Decidual infiltration of FoxP3(+) regulatory T cells, CD3(+) T cells, CD56(+) decidual natural killer cells and Ki-67 trophoblast cells in hydatidiform mole compared to normal and ectopic pregnancies, Mol. Med. Rep. 5 (1) (2012) 275–281.